Hydrogen sorption in the LiH-LiF-MgB2 system

I. Saldan;M. Schulze;C. Pistidda;R. Gosalawit-Utke;O. Zavorotynska;L. Rude;J. Skibsted;D. Haase;Y. Cerenius;T. Jensen;G. Spoto;M. Baricco;K. Taube;M. Dornheim. Hydrogen sorption in the LiH-LiF-MgB2 system. JOURNAL OF PHYSICAL CHEMISTRY. C, NANOMATERIALS AND INTERFACES. 117 pp: 17360-17366.
DOI: 10.1021/jp405856s

Hydrogen Sorption in the LiH−LiF−MgB_2 System

Ivan Saldan,*[,†,□] Matthias Schulze,[‡] Claudio Pistidda,[†] Rapee Gosalawit-Utke,[†,§] Olena Zavorotynska,[∥,⊥] Line H. Rude, Jørgen Skibsted, Dorthe Haase, Yngve Cerenius, Torben R. Jensen, Giuseppe Spoto,[∥] Marcello Baricco,[∥] Klaus Taube,[†] and Martin Dornheim[†]

[†]Helmholtz-Zentrum Geesthacht, Institute of Materials Research, Department of Nanotechnology, Max-Planck Str. 1, D-21502 Geesthacht, Germany
[‡]Helmut-Schmidt-Universitat¨University of the Federal Armed Forces Hamburg, Holstenhofweg 85, 22043 Hamburg, Germany
[§]School of Chemistry, Institute of Science, Suranaree University of Technology, Nakhon Ratchasima 30000, Thailand
[∥]Dipartimento di Chimica IFM, Universitàdi Torino and NIS, Nanostructured Interfaces and Surfaces Centre of Excellence, Via P. Giuria 7, I - 10125 Torino, Italy
[⊥]Physics Department, Institute for Energy Technology, Instituttveien 18, NO-2007 Kjeller, Norway
[#]Center for Materials Crystallography, Department of Chemistry, and Interdisciplinary Nanoscience Center (iNANO), Aarhus University, Langelandsgade 140, DK-8000 Aarhus C, Denmark
[▽]Instrument Centre for Solid-State NMR Spectroscopy, Department of Chemistry, and Interdisciplinary Nanoscience Center (iNANO), Aarhus University, Langelandsgade 140, DK-8000 Aarhus C, Denmark
[○]MAX IV Laboratory, Lund University, Ole Romers Vag 1, SE-22363 Lund, Sweden

ABSTRACT: A composite material in the LiH−LiF−MgB_2 system has been synthesized by high-energy ball milling. Some peaks in addition to that of the binary 2LiH−MgB_2 and 2LiF−MgB_2 systems are observed for the composite material by high-pressure differential scanning calorimetry (HP-DSC), indicating the formation of intermediate phases. In situ synchrotron radiation powder X-ray diffraction (SR-PXD) performed at 60 bar of H_2 and 390 °C shows a superposition of both reaction pathways that are typical for 2LiH− MgB_2 and 2LiF−MgB_2. After hydrogen absorption of the LiH−LiF− MgB_2 composite the vibrational modes of $LiBH_4$ were observed by attenuated total reflection infrared (ATR-IR) spectroscopy. The ^{19}F MAS NMR spectrum of the LiF−$LiBH_4$ sample after heat treatment in hydrogen is strongly dominated by the centerband and spinning sidebands from LiF; in addition, a low-intensity resonance, very similar to that of $[BF_4]^-$ ion, is identified.

1. INTRODUCTION

Destabilization of thermodynamically stable $LiBH_4$ for hydro-gen storage[1] by using mixtures of hydrides was first proposed and studied by the groups of Vajo et al.[2−4] at HRL Laboratories and Cho et al.[5] and Dornheim et al.[6−11] at HZG independently. The idea is to add another high capacity hydride to $LiBH_4$, so that during dehydrogenation a new stable phase or compound is formed via an exothermic reaction at a temperature which is lower than the respective decomposition temperature of pure $LiBH_4$ and therewith decreasing the desorption reaction temperature as well as the overall reaction enthalpy. Never-theless, the total gravimetric hydrogen capacity of a new composite had to be maintained at the same level. A prominent example of such reactive hydride composites (RHCs) with high gravimetric hydrogen storage density is the reversible system $LiBH_4$−MgH_2. The total enthalpy of reaction between 2 mol of $LiBH_4$ and 1 mol of MgH_2 was predicted to be about 40.5 kJ/ mol H_2 at 1 bar equilibrium pressure and 225 °C.[2] Simultaneous desorption of H_2 from $LiBH_4$ and formation of MgB_2 took place at T ≈ 400 °C and a hydrogen back pressure around 5 bar.[11] Mechanically milled mixtures of $LiBH_4$ with MgH_2 in 2:1 molar ratio were shown to store reversibly above ∼9 H_{wt}% of hydrogen. Strong influences of stoichiometry between $LiBD_4$ and MgD_2 on the reaction pathway and cycling kinetics were observed in ref 12. There it was shown that the high $LiBD_4$ content material may result in the encapsulation of MgD_2 within the LiD matrix, hindering the mass transport required for complete reaction.

Another approach to destabilize $LiBH_4$ could be the distortion of the B−H bonds inside the $[BH_4]^-$ anion by partial substitution of hydrogen atoms. Brinks et al.[13] and Eigen et al.[14] were the first who discovered the formation of mixed $NaAlH_xF_{4-x}$ phases with reduced heat of reaction if compared to the pure complex hydride. On the basis of thermodynamic modeling of solid solutions between the low-temperature phase of $LiBH_4$ and $LiBF_4$,[15] it was concluded that there are no mixed $LiBH_{4-x}F_x$ compounds stable at room temperature and 1 bar of pressure. In another theoretical work decomposition of $Li_8B_8H_{32-x}F_x$ and formation of $Li_8H_{8-x}F_x$ ($0 \le x \le 4$) compounds were proposed by first-principles calculations.[16]

In practice fluorine substitution for hydrogen in the LiH and $LiBH_4$ was reported in several experimental studies.[17,18] The first paper where authors suggest a significant destabilization with respect to pure $LiBH_4$ was shown for hydrogen absorption−desorption in the LiF−MgB_2 composite with molar ratio 2:1,[19] which was explained by the formation of MgF_2 and $LiBH_{4-x}F_x$ during hydrogenation. However, in another experimental work the main products of the hydrogen sorption were found to be MgF_2 and $LiBH_4$ even with different stoichiometry between LiF and MgB_2.[20] The LiF−MgB_2 composite with molar ratio 1:1 showed improved kinetics and good reversibility and lower hydrogen storage capacity with regard to that with molar ratio 2:1.

In this work we present a study of the new LiH−LiF−MgB_2 system. The comparison of the last to LiH−MgB_2 and LiF− MgB_2 was made. The mechanism of reversible hydrogen absorption−desorption of the prepared LiH−LiF−MgB_2 composite is discussed based on the SR-PXD, HP-DSC, ATR-IR, and NMR results.

2. EXPERIMENTAL METHODS

LiH (≥95%, Sigma Aldrich), LiF (99.99%, Sigma Aldrich), and MgB_2 (>96%, Alfa Aesar) powders were mixed by a molar ratio 1:1:1. The mixtures of powders were high-energy milled for 5 h using Spex 8000 M Mixer Mill in argon atmosphere. Stainless steel balls 10 mm in size and weight ratio to powders of 10:1 were used.

Hydrogen sorption measurements were carried out in a commercial Sievert's type apparatus (PCTpro 2000). Milled samples were hydrogenated at 60 bar of hydrogen pressure and 390 °C in a special high-pressure−temperature sample holder. The hydrogen desorption measurements were performed at 5 bar back pressure of hydrogen and 420 °C.

High pressure differential scanning calorimetry (HP-DSC) measurements were performed using a Netzsch DSC 204 HP Phoenix located in a glovebox filled with Ar. All prepared composites were heated from 25 to 530 °C using a heating rate of 5 °C/min and after that cooled to room temperature. A constant hydrogen flow of 20 mL/min was used to establish a constant pressure under hydrogen absorption/desorption at 50 or 5 bar, respectively.

In situ synchrotron radiation powder X-ray diffraction (SR-PXD) was performed at the I711 beamline of MAX II Synchrotron in Lund, Sweden.[21] A Mar165 charge-coupled detector (CCD) was exposed for 20 s with a selected X-ray wavelength of 1.07200 or 0.94608 Å for different measure-ments. The samples were airtight encapsulated in sapphire capillaries and installed in a special in situ SR-PXD cell (details described in ref 22). Samples after the third hydrogen desorption were heated with 5 °C min rate from room temperature up to 390 °C and kept at isothermal conditions for 1 h under 60 bar of H_2. After that they were cooled to room temperature in open air. All handling and preparation of materials took place in a glovebox with continuously purified argon atmosphere and oxygen, and moisture values were less than 1 ppm.

Attenuated total reflection infrared (ATR-IR) spectra were taken on a Bruker-ALPHA Platinum spectrometer with ATR diamond crystal accessory. The spectra were recorded in the 4000−375 cm^{-1} range with 2 cm^{-1} resolution. Sixty-four scans were averaged for background and sample spectra. All the measurements were carried out at room temperature in the nitrogen-filled glovebox with O_2 and H_2O levels less that 1 ppm.

Solid-state ^{11}B and ^{19}F MAS NMR spectra were acquired for samples of $LiBH_4$ mixed with LiF in a 1:1 molar ratio. The mixture was milled for 25 h using a planetary Mill (Fritsch-Pulverisette 5) under 250 rpm in argon atmosphere. A ceramic vial and 10 mm ceramic balls with ball to powder ratio of 10:1 were used. The samples were heat treated in a commercial Sievert's type apparatus PCTpro 2000 in a vacuum (P ∼ 0.05 bar; T = 390 °C; 23 h) or hydrogen atmosphere (P ∼ 60 bar H_2; T = 390 °C; 3 h). The ^{11}B and ^{19}F MAS NMR spectra were obtained at room temperature on Varian INOVA-400 (9.39 T) and Varian INOVA-300 (7.05 T) spectrometers, respectively, using home-built CP/MAS NMR probes for 5 mm o.d. Si_3N_4 rotors (110 μL sample volume). The samples were loaded in the PSZ rotors in an argon-filled glovebox and closed using Torlon end-caps equipped with two Viton o-rings. The ^{11}B and ^{19}F chemical shifts are referenced to neat $F_3B{\cdot}O(CH_2CH_3)_2$ and $CFCl_3$, respectively.

3. RESULTS AND DISCUSSION

3.1. Hydrogen Uptake−Release Cycles of the LiH− LiF−MgB_2 Composite. The LiH−LiF−MgB_2 hydrogenation at 60 bar of hydrogen pressure and 390 °C as well as dehydrogenation at 5 bar back pressure and 420 °C were performed for approximately 50 h in the case of the first cycle (Figure 1). The first hydrogen uptake and release cycle acts as activation for the next ones which might be explained by grain refinement in the solid composite under cycling. The kinetics of the second and third cycles were very similar to that of the LiF−MgB_2 composite with molar ratio 2:1,[20] but no incubation period was observed for LiH−LiF−MgB_2. Probably this fact is explained by fast nucleation of MgB_2 because of the small lattice misfit between MgB_2 and LiH as shown in ref 9. Only because of the absence of this incubation period in the LiH− LiF−MgB_2 composite the kinetics of hydrogen sorption can be regarded as improved compared to 2LiF−MgB_2. Since LiH has three times lower weight than LiF, the theoretical gravimetric hydrogen storage capacity in the LiF−LiH−MgB_2 composite is 9.2 wt % H_2 and therefore higher than that of 2LiF−MgB_2 (7.5 wt % H_2). Hydrogen uptake by the LiH−LiF−MgB_2 composite was measured as ∼7.0, 7.0, and 6.7 wt % H_2 for the first, second, and third cycle, respectively (Figure 1a). In the case of desorption (Figure 1b) in contrast to subsequent cycles, the first cycle did not show the full reversible hydrogen capacity (∼5.6 wt % H_2). In accordance with the 2LiF−MgB_2 case published in ref 20 only for the first cycle three stages of hydrogen absorption or desorption could be distinguished. For LiH−LiF−MgB_2 these stages are: 0−3, 3−18, and 18−50 h. The following cycles were smoother and quite reproducible. It can be concluded that adding of LiH to the LiF−MgB_2 system indeed increases hydrogen storage capacity from 6.4 wt % H_2 (for 2LiF−MgB_2) to 7.0 wt % H_2 (for LiH−LiF−MgB_2) and eliminates the incubation period during the hydrogen desorption.

3.2. Differential Scanning Calorimetry of the LiH− LiF−MgB_2 Composite under Hydrogen Absorption Desorption. For the LiH−LiF−MgB_2 composite HP-DSC measurements for hydrogen uptake and subsequent release were performed (Figure 2). Phase transformation and melting-solidification of $LiBH_4$ (peaks A and B, respectively) correspond to those temperatures given in ref 20 for LiF− MgB_2 composites. During hydrogen absorption a broad exothermic peak appeared approximately from 100 to 400 °C (Figure 2a). In the case of hydrogen release during heating, in addition to the typical (A) and (B) endothermic peaks, MgH_2 decomposition (C) at ∼360 °C and further decomposition of $LiBH_4$ (E) at ∼500 °C were visible together with two unknown events (D) in the temperature region 450−460 °C (Figure 2b). Probably, both (D) and (E) peaks are responsible for hydrogen desorption from the $LiBH_4$ since the peak position of (E) is very similar to that in LiF−MgB_2 composites,[20] but its intensity is much lower. We suggest that (D) events might be some intermediates under $LiBH_4$ decomposition which could appear again under cooling at (F).

In conclusion, HP-DSC of the LiH−LiF−MgB_2 composite under hydrogen sorption showed new events that could be the signal of hydrogen release from intermediates. It means that the reaction pathway in the LiH−LiF−MgB_2 might be different from the LiF−MgB_2 system.

3.3. In Situ SR-PXD of the Dehydrogenated LiH−LiF− MgB_2 Composite under Hydrogen Absorption. To understand the reaction mechanism of hydrogen sorption in the LiH−LiF−MgB_2 composite an in situ SR-PXD measure-ment was performed after the third desorption (Figure 3). The results showed that after the third hydrogen desorption LiH, LiF, and MgB_2 together with pure Mg were present in the sample. As was mentioned in ref 11 the products of the hydrogen desorption reaction of 2$LiBH_4$−MgH_2 strongly depend on hydrogen pressure and applied temperature. At low pressures and high temperatures (T ≥ 450 °C and P ≤ 3 bar) amorphous boron and pure magnesium can be formed by the reaction[11]

$$2LiBH_4 + MgH_2 \leftrightarrow 2LiH + Mg + 2B + 4H_2 \quad (1)$$

During heating at 60 bar of H_2 the dehydrogenated LiH− LiF−MgB_2 composite started to absorb hydrogen at ∼360 °C, which is evident by the emerging of the peaks due to MgH_2 and MgF_2. At this temperature $LiBH_4$ is liquid, but the peaks due to the crystalline $LiBH_4$ became evident during cooling at around 100 °C. Therefore a presumable hydrogenation reaction path omitting any possible intermediates might be

$$LiF + LiH + MgB_2 + 4H_2 \leftrightarrow 2LiBH_4 + 1/2MgF_2 + 1/2MgH_2 \quad (2)$$

As it was mentioned before in Section 3.1 the experimental hydrogen storage capacity of this composite is around 7 wt % H_2 which is in good agreement with the calculated (∼9.2 wt % H_2) value according to eq 2. In addition to the products of hydrogen absorption Li_2B_6 was also detected. This new phase appeared during the isothermal period and remained even at room temperature. Probably at high temperature amorphous B, formed by eq 1, reacted with LiF and/or LiH together with MgB_2 by the chemical reaction

$$LiF + LiH + MgB_2 + 4B \rightarrow Li_2B_6 + 1/2MgH_2 + 1/2MgF_2 \quad (3)$$

In conclusion, the mechanism of hydrogen sorption of LiH− LiF−MgB_2 composite (eq 2) was suggested based on in situ SR-PXD measurement. The results showed a superposition of two processes typical for 2LiH−MgB_2[11] and 2LiF−MgB_2[20] composites. Small amounts of pure Mg and Li_2B_6 obviously appeared by reactions 1 and 3, correspondently, giving evidence of a strong pathway dependence on the pressure and applied temperature.

3.4. Attenuated Total Reflection Infrared Spectrosco-py of the LiH−LiF−MgB_2 Composite. ATR-IR spectroscopy was used to characterize the composites before and after hydrogen absorption since the formation of the compounds with complex anions, such as $[BH_4]^-$, $[BF_4]^-$, or even $[BH_{4-x}F_x]^-$, can be easily seen in the IR spectra. Furthermore, the vibrational features of these anions depend on their symmetry and therefore on the crystal lattice they are embedded in. The ATR-IR spectra of the LiH−LiF−MgB_2 composite after ball-milling and third hydrogen desorption are shown in Figure 4. It is readily seen that these spectra do not exhibit the characteristic modes of B−H stretching and H−B− H bending in the 2400−2000 and 1400−900 cm^{-1} region.[23] Instead, the spectra of the composite have the baselines steadily increasing in absorption at the lower frequencies due to the lattice phonons of the compounds like, for example, LiF, LiH, or MgB_2.

The ATR-IR spectrum of the LiH−LiF−MgB_2 composite after the first hydrogen absorption is shown in Figure 5. The characteristic $[BH_4]^-$ vibrational profile in $LiBH_4$ with B−H stretching and H−B−H bending modes, respectively, in the 2400−2000 and 1400−900 cm^{-1} regions is observable.[23] In general, the spectrum of $LiBH_4$ formed in the hydrogenated mixture is similar to that of the commercially available $LiBH_4$, where the different components of $\tilde{\nu}_2$,$\tilde{\nu}_3$,and $\tilde{\nu}_4$normal modes can be distinguished. Since no modifications of the $[BH_4]^-$ vibrations are observable in the spectrum of hydrogenated LiH−LiF−MgB_2, the formation of $LiBH_{4-x}F_x$ phases is not evidenced. The additional broad peak at ca. 1000 cm^{-1}, however, is present. It can correspond to the B−F stretching vibrations, pointing at the formation of some B−F containing groups. At the same time, the peak due to F−B−F bending in the $[BF_4]^-$ groups, present at ca. 550 cm^{-1} in the reference spectrum of $LiBF_4$, is not visible in the spectrum of the hydrogenated LiH−LiF−MgB_2 composite; therefore, these anions could not be detected in the sample.

3.5. Investigation of Possible Fluoride Substitution Using ATR-IR and ^{11}B and ^{19}F MAS NMR Spectroscopy.
Several experimental studies have reported a significant destabilization of $LiBH_4$ by fluoride substitution.[17−19] To study whether fluoride substitution occurs between LiF and $LiBH_4$ in the LiH−LiF−MgB_2 composite system, a ball-milled sample of $LiBH_4$−LiF has been studied by ATR-IR. The sample was subsequently exposed to heat treatment in either hydrogen atmosphere (T = 390 °C, 60 bar of H_2) or vacuum (T = 390 °C, ∼0.05 bar), and both samples were studied by ^{11}B and ^{19}F
MAS NMR.

The ATR-IR spectrum of the $LiBH_4$−LiF system after ball milling is compared with the corresponding spectra of commercial LiF and $LiBH_4$ in Figure 6. The IR spectrum of the $LiBH_4$−LiF sample after ball milling shows the presence of a physical mixture of $LiBH_4$ and LiF, and no fluoride substitution is observed.

The ^{11}B MAS NMR spectra of the ball-milled LiF−$LiBH_4$ sample exposed to heat treatment in a hydrogen atmosphere and in vacuum are compared in Figure 7. The ^{11}B MAS NMR spectrum of the sample stored in hydrogen (Figure 7a) is identical to the spectrum after ball-milling (not shown) and shows the characteristic spectrum for the ^{11}B central and satellite transitions for $LiBH_4$,[24] with the isotropic chemical shift $\delta(^{11}B)$ = −41.2 ppm. Furthermore, low-intensity resonances in the range of $\delta(^{11}B)$ = 18−1 ppm are observed, which most likely arise from a small amount of borate species, BO_3 and BO_4 units,[25] formed as impurities as a result of reaction with oxygen during the preparation/handling of the sample. After heat treatment in vacuum (Figure 7b), a significant amount of $LiBH_4$ has decomposed and formed amorphous boron (α-B) as observed by the broad centerband resonance at $\delta(^{11}B) \approx 0$ ppm. A very small resonance at 1.4 ppm remains in the spectrum and indicates a small impurity of BO_4 species. The ^{11}B resonance for a commercial sample of $LiBF_4$ is observed at $\delta(^{11}B)$ = −2.8 ppm, and thus, we expect that ^{11}B resonances from $LiBH_{4-x}F_x$ should fall in the range −2 to −41.2 ppm. However, no additional resonances are observed in this range for the two heat-treated samples, indicating that no or only a very small degree of F^- substitution into $LiBH_4$ has occurred for the two samples.

The ^{19}F MAS NMR spectra of commercial LiF and the two heat-treated LiF−$LiBH_4$ samples are compared in Figure.8. A ^{19}F centerband resonance at $\delta(^{19}F)$ = −202.8 ppm is observed for commercial LiF (Figure 8a), flanked by a number of spinning sidebands with significant intensity, which reflect strong ^{19}F−^{19}F dipolar couplings. The ^{19}F MAS NMR spectrum of the LiF−$LiBH_4$ sample after heat treatment in hydrogen (Figure 8b) is quite similar and thereby demonstrates that fluorine is mainly present as LiF. However, a high-frequency shoulder (asterisk) is observed for the first-order spinning sideband from LiF, showing the presence of a second fluorine-containing phase. This resonance is more clearly observed in the difference spectrum between Figure 8b and Figure 8a, which shows a narrow peak at $\delta(^{19}F)$ = −159.2 ppm. The chemical shift for this resonance is very similar to the value $\delta(^{19}F)$ = −162.4 ppm, observed under the same experimental conditions for a commercial sample of $LiBF_4$. Thus, the observation of this resonance strongly suggests that a small degree of fluoride

substitution in $LiBH_4$ has taken place for the $LiF-LiBH_4$ sample. However, the degree of fluoride sub-stitution is so small that it is not clearly observed by ^{11}B NMR; i.e., the corresponding low-intensity ^{11}B resonance may be blurred by overlap with the resonances from either $LiBH_4$ or the BO_4 impurity. However, a very small ^{11}B centerband resonance is observed at $\delta(^{11}B) = -15$ ppm which may originate from $BH_{4-x}F_x$ units. The small shift (3 ppm) of the ^{19}F peak, relative to the resonance from pure $LiBF_4$, suggests that the $LiF-LiBH_4$ sample after heat treatment in hydrogen contains a small fraction of $BH_{4-x}F_x$ units, most likely BH_3F^- units, rather than BF_4^- anions.

The ^{19}F MAS NMR spectrum of the sample exposed to heat treatment under vacuum (Figure 8c) shows only the presence of LiF in the sample, and the −159 ppm peak cannot be identified in difference plots between Figure 8c and Figure 8a.

The first results of near-edge X-ray absorption fine structure (NEXAFS) at the B K-edge (193 eV) for the $LiF-MgB_2$ composite with molar ratio (2:1) are presented in the recent paper.[26] The obtained results indicate the formation of mixed borohydrides/borofluorides of the type of $LiBH_{4-x}F_x$, thus suggesting fluorine substituting for hydrogen inside the $[BH_4]^-$ anion. In addition to that, the conclusion about the substitution based on the ^{19}F MAS NMR spectrum of the $LiF-LiBH_4$ sample after heat treatment in hydrogen is a second strong hint that has been made in the present paper. Apparently, compared to SR-PXD, HP-DSC, and ATR-IR, the NMR and XAFS spectroscopies might be more sensitive to identify $LiBH_{4-x}F_x$-type phases. Therefore, all systems ($LiF-MgB_2$, $LiH-LiF-MgB_2$, and $LiF-LiBH_4$) are recommended to be analyzed by ^{19}F MAS NMR and XAFS at the B K-edge.

4. CONCLUSIONS

Hydrogen absorption capacity of the $LiH-LiF-MgB_2$ composite was estimated as ∼7.0, 7.0, and 6.7 wt % H_2 correspondently for the first, second, and third cycle, which is higher than that of $2LiF-MgB_2$.[20] Incubation periods which are present in $2LiF-MgB_2$ composites were not observed for hydrogen sorption of the $LiH-LiF-MgB_2$. Only because of the absence of this incubation period in $LiH-LiF-MgB_2$ the kinetics of hydrogen sorption with regard to $2LiF-MgB_2$ can be improved, whereas with comparison to $2LiH-MgB_2$ is slower.[9]

During hydrogen absorption HP-DSC characterization of the $LiH-LiF-MgB_2$ composite was similar to that of $2LiF-MgB_2$.[18] In the case of hydrogen desorption endothermic peaks of MgH_2 and $LiBH_4$ decomposition were visible together with two unknown events. We suggest that these new peaks might be signals of some intermediates under $LiBH_4$ decomposition which could be reversible under cooling.

No crystalline compounds as intermediates of $LiBH_4$ decomposition were detected using in situ SR-PXD measure-ment. During hydrogen sorption of the $LiH-LiF-MgB_2$ composite, MgH_2, $LiBH_4$, and MgF_2 were found as the main reaction products. In addition to these, small amounts of pure Mg and Li_2B_6 confirmed additional reactions under a hydrogen uptake-release cycling.

The ex situ ATR-IR spectra of the $LiH-LiF-MgB_2$ composite as milled and after the third hydrogen desorption did not show the peaks due to the $LiBH_4$, but after hydrogen absorption the vibrational modes essentially identical to that of the commercial $LiBH_4$ were found. The ATR-IR spectrum of a $LiBH_4-LiF$ sample after ball milling shows the presence of a physical mixture of $LiBH_4$ and LiF.

The ^{11}B MAS NMR spectrum of the $LiBH_4-LiF$ sample after heat treatment in hydrogen (T = 390 °C; 60 bar H_2) showed the presence of $LiBH_4$ along with a small impurity of borate species (BO_3 or BO_4). After heat treatment in vacuum (T = 390 °C; ∼0.05 bar), a significant amount of $LiBH_4$ has decomposed, and amorphous boron was formed. The ^{19}F MAS NMR spectrum of the $LiBH_4-LiF$ sample after heat treatment in hydrogen is strongly dominated by the resonances from LiF; however, a second fluoride-containing phase has also been identified, where the close similarity in ^{19}F chemical shift with $LiBF_4$ strongly suggests that this phase includes the $[BF_4]^-$ ion. However, the amount of this F-anion substitution in $LiBH_4$ is too small to be used to alter the thermodynamics of $LiBH_4-MgH_2$ composites significantly.

ACKNOWLEDGMENTS

The research leading to these results has received funding from the European Community's Seventh Framework Programme FP 7/2007-2013 under grant agreement # 226943-FLYHY.

The use of the facilities at the Instrument Centre for Solid-State NMR Spectroscopy, Department of Chemistry, Aarhus University, sponsored by the Danish Natural Science Research Council, the Danish Technical Science Research Council, Teknologistyrelsen, Carlsbergfondet, and Direktør Ib Henrik-sens Fond, is acknowledged.

REFERENCES

(1) Smith, M. S.; Bass, G. E. Heats and Free Energies of Formation of the Alkali Aluminum Hydrides and of Cesium Hydride. J. Chem. Eng. Data 1963, 8, 342−346.
(2) Vajo, J.; Skeith, S.; Mertens, F. Reversible Storage of Hydrogen in Destabilized $LiBH_4$. J. Phys. Chem. B 2005, 109, 3719−3722.
(3) Vajo, J.; Olson, G. L. Hydrogen Storage in Destabilized Chemical Systems. Scr. Mater. 2007, 56, 829−834.
(4) Vajo, J.; Salguero, T. T.; Gross, A. F.; Skeith, S. L.; Olson, G. L. Thermodynamic Destabilization and Reaction Kinetics in Light Metal Hydride Systems. J. Alloys Compd. 2007, 446−447, 409−414.
(5) Cho, Y. W.; Shim, J. H.; Lee, B. J. Thermal Destabilization of Binary and Complex Metal Hydrides by Chemical Reaction: A Thermodynamic Analysis. CALPHAD 2006, 30, 65−69.
(6) Barkhordarian, G.; Klassen, T.; Dornheim, M.; Bormann, R.Unexpected Kinetic Effect of MgB_2 in Reactive Hydride Composites Containing Complex Borohydrides. J. Alloys Compd. 2007, 440, L18− L21.
(7) Dornheim, M.; Doppiu, S.; Barkhordarian, G.; Bösenberg, U.; Klassen, T.; Gutfleisch, O.; Bormann, R. Hydrogen Storage in Mg-Based Hydrides and Hydride Composites. Scr. Mater. 2007, 56, 841− 846.
(8) Bosenberg, U.; Doppiu, S.; Mosegaard, L.; Barkhordarian, G.;Eigen, N.; Borgschulte, A.; Jensen, T. R.; Cerenius, Y.; Gutfleisch, O.; Klassen, T.; Dornheim, M.; Bormann, R. Hydrogen Sorption Properties of $MgH_2 + 2LiBH_4$. Acta Mater. 2007, 55, 3951−3958.
(9) Bösenberg, U.; Kim, J. W.; Gosslar, D.; Eigen, N.; Jensen, T. R.; Bellosta Von Colbe, J. M.; Zhou, Y.; Dahms, M.; Kim, D. H.; Günther, R.; Cho, Y. W.; Oh, K. H.; Klassen, T.; Bormann, R.; Dornheim, M. Role of Additives in $LiBH_4-MgH_2$ Reactive Hydride Composites for Sorption Kinetics. Acta Mater. 2010, 58, 3381−3389.

(10) Nielsen, T. K.; Bösenberg, U.; Gosalawit, R.; Dornheim, M.;Cerenius, Y.; Besenbacher, F.; Jensen, T. R. A Reversible Nano-confined Chemical Reaction. ACS Nano 2010, 4, 3903−3908.
(11) Bösenberg, U.; Ravnsbæk, D. B.; Hagemman, H.; D'Anna, V.; Bonatto Minella, Ch.; Pistidda, C.; Wouter van Beek, Jensen, T. R.; Cerenius, Y.; Gutfleisch, O.; Bormann, R.; Dornheim, M. Pressure and Temperature Influence on the Desorption Pathway of the $LiBH_4$− MgH_2 Composite System. J. Phys. Chem. C 2010, 114, 15212−15217.
(12) Price, T. E. C.; Grant, D. M.; Legrand, V.; Walker, G. S.Enhanced Kinetics for the $LiBH_4$:MgH_2 Multi-Component Hydrogen Storage System - the Effects of Stoichiometry and Decomposition Environment on Cycling Behavior. J. Hydrogen Energy 2010, 35, 4154−5161.
(13) Brinks, H. W.; Fossdal, A.; Hauback, B. C. Adjustment of the Stability of Complex Hydrides by Anion Substitution. J. Phys. Chem. C 2008, 112, 5658−5661.
(14) Eigen, N.; Bösenberg, U.; Bellosta von Colbe, J.; Jensen, T. R.;Cerenius, Y.; Dornheim, M.; Klassen, T.; Bormann, R. Reversible Hydrogen Storage In Naf−Al Composites. J. Alloys Compd. 2009, 477, 76−80.
(15) Corno, M.; Pinatel, E.; Ugliengo, P.; Baricco, M. A Computational Study on the Effect of Fluorine Substitution in $LiBH_4$. J. Alloys Compd. 2011, 509, 679−683.
(16) Yin, L.; Wang, P.; Fang, Zh.; Cheng, H. Thermodynamically Tuning of $LiBH_4$ by Fluorine Anion Doping for Hydrogen Storage: a Density Functional Study. Chem. Phys. Lett. 2008, 450, 318−321.
(17) Messer, Ch. E.; Mellor, J. The System Lithim Hydride−Lithium Fluoride. J. Phys. Chem. 1960, 64, 503−505.
(18) Polenko, A. N.; Tabachnic, M. E.; Cholakh, S. O.; O'Connel-Bronin, A. A. Exciton States of Lithium Hydride in $LiH_{1-x}F_x$ Solid Solutions. Phys. Status Solidi 1993, 179, 411−418.
(19) Gosalawit, R.; Bellosta von Colbe, J. M.; Dornheim, M.; Jensen, T. R.; Cerenius, Y.; Bonatto, Ch. M.; Peschke, M.; Bormann, R. $LiBH_4$−MgH_2 System for Reversible Hydrogen Storage. J. Phys. Chem. C 2010, 114, 10291−10296.
(20) Saldan, I.; Gosalawit-Utke, R.; Pistidda, C.; Bösenberg, U.; Schulze, M.; Jensen, T. R.; Taube, K.; Dornheim, M.; Klassen, T. Influence of Stoichiometry on the Hydrogen Sorption Behavior in the LiF−MgB_2 System. J. Phys. Chem. C 2012, 116, 7010−7015.
(21) Cerenius, Y.; Stahl, K.; Svesson, L.; Ursby, T.; Oskarsson, Å.; Albertsson, J. The Crystallographic Beamline I711 at MAX II. J. Synchrotron Radiat. 2000, 7, 203−208.
(22) Jensen, T. R.; Nielsen, T. K.; Filinchuk, Ya.; Jørgensen, J. E.; Cerenius, Y.; Gray, E. M.; Webb, C. J. Versatile in Situ Powder X-ray Diffraction Cells for Solid-Gas Investigations. J. Appl. Crystallogr. 2010, 43, 1456−1463.
(23) Zavorotynska, O.; Corno, M.; Damin, A.; Spoto, G.; Ugliengo, P.; Baricco, M. Vibrational Properties of MBH_4 and MBF_4 Crystals (M = Li, Na, K): a Combined DFT, Infrared, and Raman Study. J. Phys. Chem. C 2011, 115, 18890−18900.
(24) Arnbjerg, L. M.; Ravnsbæk, D. B.; Filinchuk, Y.; Vang, R. T.; Cerenius, Y.; Besenbacher, F.; Jørgensen, J. E.; Jakobsen, H. J.; Jensen, T. R. Structure and Dynamics for $LiBH_4$−LiCl Solid Solutions. Chem. Mater. 2009, 21, 5772−5782.
(25) Hansen, M. R.; Vosegaard, T.; Jakobsen, H. J.; Skibsted, J. ^{11}B Chemical Shift Anisotropies in Borates from ^{11}B MAS, MQMAS, and Single-Crystal NMR Spectroscopy. J. Phys. Chem. A 2004, 108, 586− 594.
(26) Saldan, I.; Ramallo-Lopez, J. M.; Requejo, F. G.; Suarez-Alcantara, K.; Bellosta von Colbe, J.; Avila, J. NEXAFS Study of 2LiF−MgB_2 Composite. J. Hydrogen Energy 2012, 37, 10236−10239.

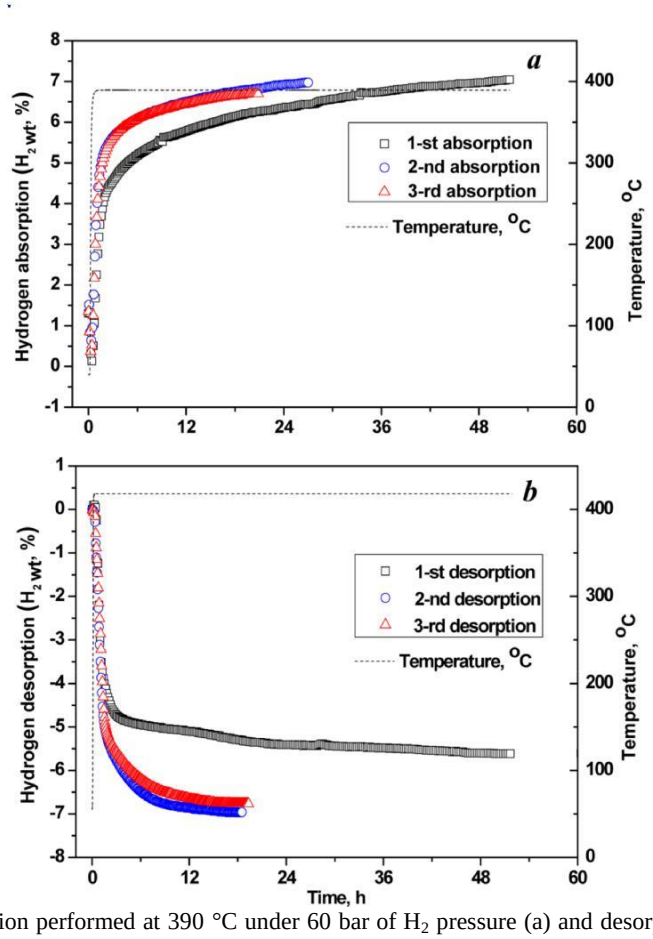

Figure 1. Hydrogen absorption performed at 390 °C under 60 bar of H_2 pressure (a) and desorption at 420 °C under 5 bar of H_2 (b) for the LiH−LiF−MgB_2 composite with molar ratio 1:1:1.

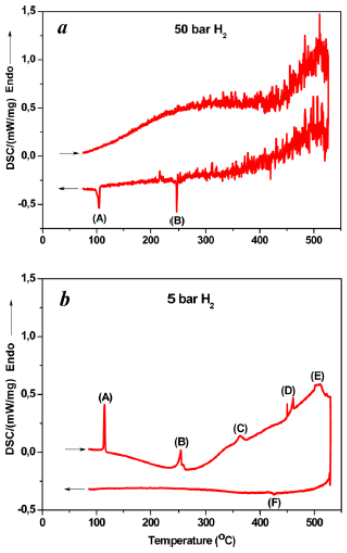

Figure 2. HP-DSC investigation (heating/cooling rate of 5 °C/min) for the LiH−LiF−MgB_2 composite with molar ratio 1:1:1 at hydrogen absorption (a) and desorption (b). (A) Peak position corresponds to the $LiBH_4$ phase transformation. (B) Melting-solidification of $LiBH_4$. (C) Decomposition of MgH_2. (D) Unknown event. (E) Decom-position of $LiBH_4$. (F)Unknown event. A constant hydrogen flow of 20 mL/min was used to establish a constant pressure under hydrogen absorption/desorption: 50 or 5 bar, respectively.

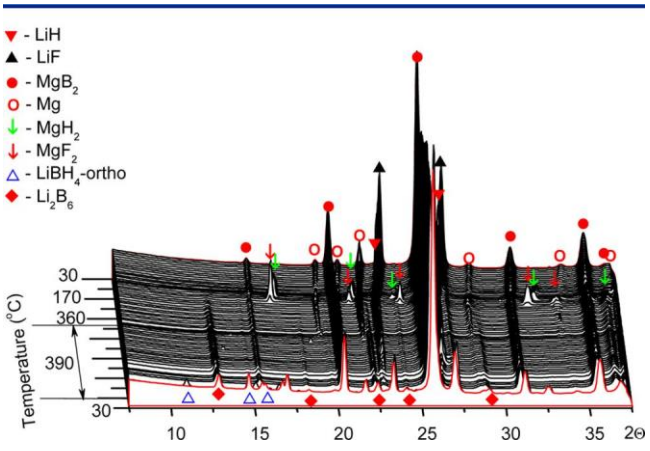

Figure 3. In situ SR-PXD performed at 60 bar of H_2 and 390 °C isothermal period for 1 h of the LiH−LiF−MgB_2 composite with molar ratio (1:1:1) after the third hydrogen desorption. The first and last patterns are in red.

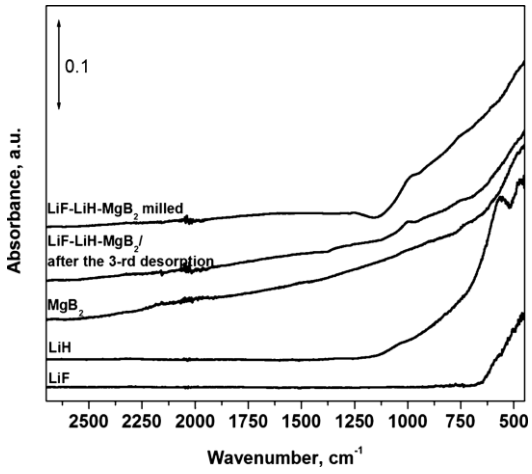

Figure 4. ATR-IR spectra of the LiH−LiF−MgB2 composite as milled and after the third hydrogen desorption. Spectra of commercial LiH, LiF, and MgB2 are shown for comparison. Spectra are translated along the y-axis for better representation.

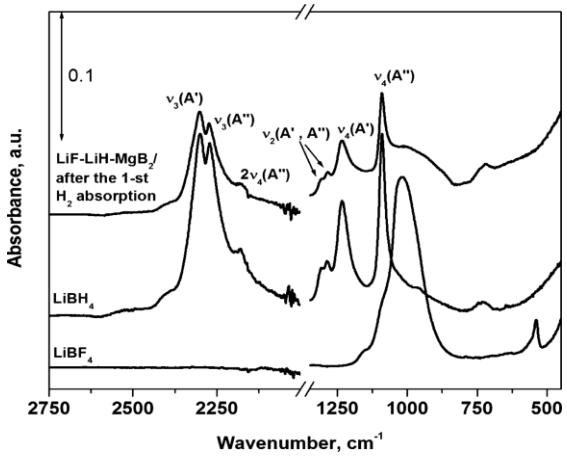

Figure 5. ATR-IR spectra of the LiH−LiF−MgB_2 composite after the first hydrogen absorption. Spectra of commercial $LiBH_4$ and $LiBF_4$ are shown for comparison. Spectra are translated along the y-axis for better representation.

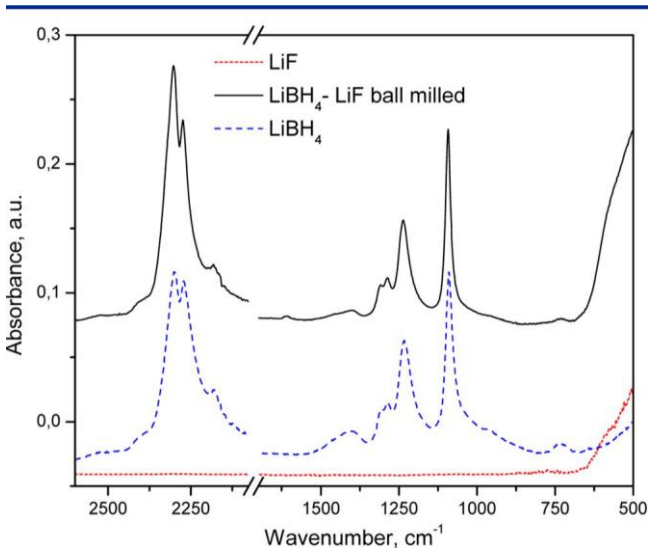

Figure 6. ATR-IR spectra of the ball-milled LiF−$LiBH_4$ composite compared with commercial LiF and $LiBH_4$.

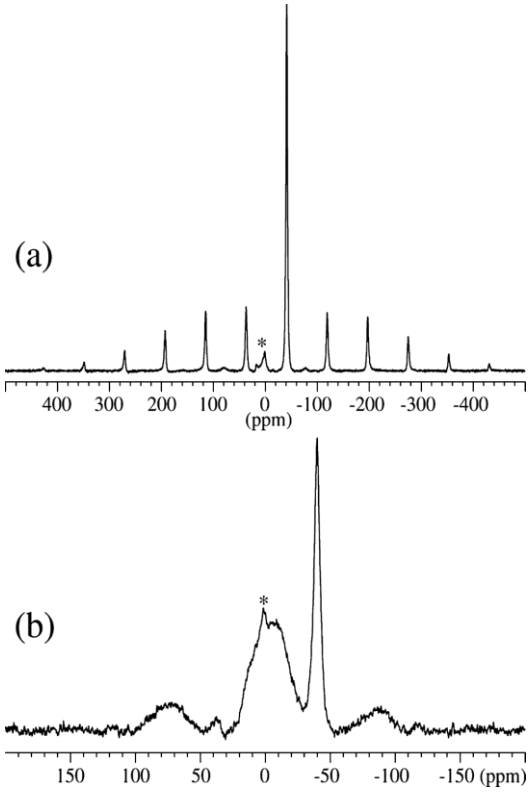

Figure 7. (a) ^{11}B MAS NMR spectrum of the central and satellite transitions for $LiBH_4$ (δ = −41.2 ppm) in the $LiBH_4$–LiF sample after heat treatment (T = 390 °C) in a hydrogen atmosphere ($P(H_2)$ = 60 bar). (b) ^{11}B MAS NMR spectrum of the central-transition region for the $LiBH_4$–LiF sample after a similar heat treatment in vacuum (~0.05 bar). A small resonance from an oxide impurity (BO4 species, δ = 1.2 ppm) is present in both spectra and is marked by an asterisk. The ^{11}B MAS NMR spectra (9.4 T) have been acquired with ^{1}H decoupling and a spinning speed of ν_R = 10.0 kHz, using a short excitation pulse (τ_p = 0.5 μs) and a relaxation delay of (a) 10 s (100 scans) and (b) 30 s (1024 scans).

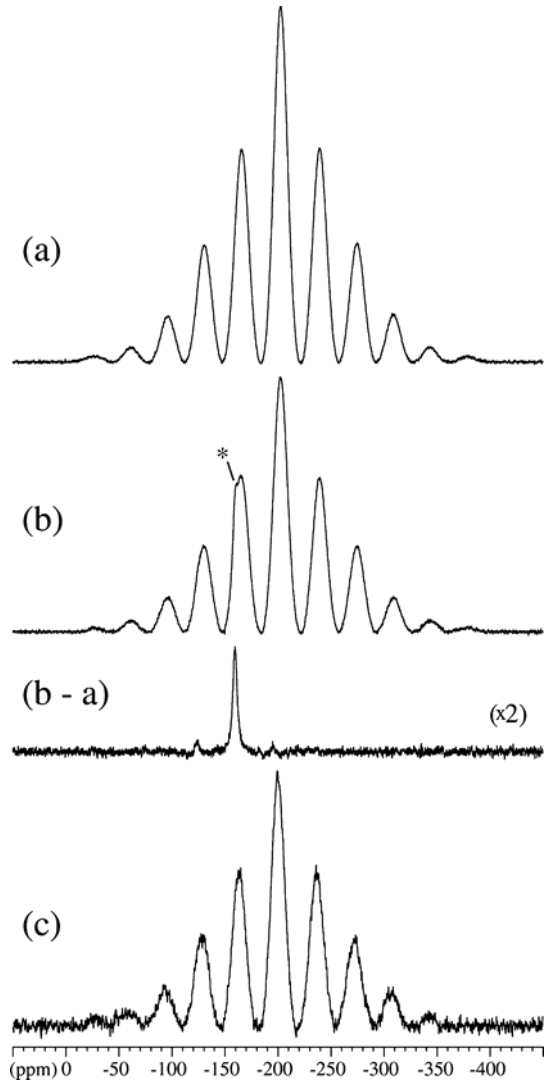

Figure 8. ^{19}F MAS NMR spectra (7.1 T, ν_R = 10.0 kHz) of (a) commercial LiF and the ball-milled $LiBH_4$–LiF sample after heat treatment (T = 390 °C) in (b) a hydrogen atmosphere ($P(H_2)$ = 60 bar) and (c) in vacuum (~0.05 bar). The asterisk in (b) indicates a second resonance, which overlaps with the first-order spinning sideband from LiF. This resonance becomes clearly apparent in the difference spectrum for (a) and (b), shown below spectrum (b). The intensity in the difference spectrum is multiplied by a factor of 2 relative to the spectrum in (b). All spectra are with a ~30° excitation pulse and a relaxation delay of 30 s. The lower S/N ratio in part (c) reflects that only a small amount of sample was available for this experiment.